ISSN 0006-2979, Biochemistry (Moscow), 2025, Vol. 90, No. 12, pp. 1999-2008 © The Author(s) 2025. This article is an open access publication.
Published in Russian in Biokhimiya, 2025, Vol. 90, No. 12, pp. 2108-2118.

Mitochondrial Lipid Peroxidation Initiates Rapid Accumulation of Lipofuscin in Cultured Cells

He Huan[1], Alisa A. Panteleeva[1], Ruben A. Simonyan[1], Armine V. Avetisyan[1], Konstantin G. Lyamzaev[1,2,a]*, and Boris V. Chernyak[1]

[1]*Belozersky Institute of Physico-Chemical Biology, Lomonosov Moscow State University, 119991 Moscow, Russia*

[2]*Russian Clinical Research Center of Gerontology, Pirogov Russian National Research Medical University, Ministry of Health of the Russian Federation, 129226 Moscow, Russia*

[a]*e-mail: lyamzaev@gmail.com*

Received August 15, 2025
Revised September 12, 2025
Accepted September 16, 2025

Abstract—Activation of lipid peroxidation (LPO) in the mitochondria of rat H9c2 cardiomyoblasts and human fibroblasts by the cystine transport inhibitor erastin or glutathione peroxidase 4 inhibitor RSL3 was accompanied by rapid (18 h) accumulation of lipofuscin. The mitochondria-targeted antioxidant SkQ1 and redox mediator methylene blue, which prevents the formation of reactive oxygen species (ROS) in the mitochondrial respiratory chain complex I, blocked both mitochondrial LPO and lipofuscin accumulation. These data indicate that mitochondrial LPO serves as a driving force for the accelerated accumulation of lipofuscin in cells. Rapid (24 h) lipofuscin formation was observed in isolated heart mitochondria in the presence of iron ions. It was significantly accelerated by ROS generated in the respiratory chain complex I and blocked by SkQ1. The question of whether oxidized components of mitochondria serve as a source for lipofuscin formation in cells remains open. The results obtained suggest possible application of mitochondria-targeted compounds in the treatment of diseases associated with excessive lipofuscin accumulation.

DOI: 10.1134/S0006297925602606

Keywords: lipid peroxidation, mitochondria, ferroptosis, lipofuscin

INTRODUCTION

Lipofuscin (LF) is insoluble pigment aggregates that accumulate in cells during aging. LF was first described by the Danish physician and histologist Adolf Hannover [1], although its association with aging had not been recognized until the late nineteenth century. LF is composed mainly of highly oxidized proteins, with smaller amounts of lipids, carbohydrates, and nucleic acids, and contains metal ions, including iron, which determines its involvement in oxidative processes [2]. The composition of LF varies considerably across different types of cells; its analysis is complicated by extensive covalent cross-linking of constituent macromolecules. In a body, LF primarily accumulates in postmitotic cells, such as neurons and cardiomyocytes. In actively phagocytizing cells, in particular, macrophages [3] and retinal pigment epithelium (RPE) cells [4], a substantial fraction of LF originates from the endocytosed material. For example, in RPE cells that phagocytize fragments of retinal-containing photoreceptors, the major LF component is a retinal dimer conjugated with ethanolamine (A2E). Accumulation of LF in RPE cells has been implicated in the development of age-related macular degeneration [5].

In cells, LF is found in the cytosol and endosomal compartments. It is believed to be generated by oxidation of various cellular constituents and delivered to the lysosomes via autophagy [6]. Once inside the lysosomes, LF is mostly resistant to degradation but may undergo modifications and even “grow” by reacting with neighboring proteins through reactive surface groups [6]. Inhibition of lysosomal proteolytic activity *in vivo* results in LF accumulation in multiple organs [7].

* To whom correspondence should be addressed.

Mitochondria have been proposed as one of the principal sources of LF [8]. Proteomic analysis of brain-derived LF [9] identified several mitochondrial proteins along with proteins from other cellular compartments, although the available data are insufficient to establish mitochondria as the primary site of LF origin. Like other protein aggregates, LF can inhibit the proteasomal activity, and its accumulation in lysosomes may impair their function. However, whether LF plays an active role in the age-related cellular damage remains unknown.

The stimulation of autophagy in aged rats reduced the LF content, which correlated with a decrease in the proportion of cardiomyocytes displaying senescence markers [10], although no causality could be reliably established in such experiments. Exogenously applied purified LF impaired the functioning of cardiomyocytes [11] and RPE cells [12] and even induced the death of fibroblasts [13]. The age-associated LF accumulation has been documented in various organs, including the heart [14]. Thus, smaller short-lived species of primates were found to display much faster LF accumulation in the heart [15]. Examination of human cardiac tissue from individuals aged 20 to 97 revealed that LF levels correlated with aging but did not depend on body weight or cause of death [16]. LF accumulation during both replicative and stress-induced senescence is a major biomarker of aging in cultured cells and is widely used in research [17].

Lipid peroxidation (LPO), in particular, oxidation of polyunsaturated fatty acids in membrane phospholipids, is a key driver of LF accumulation. Thus, iron chelators capable of penetrating into cells and suppressing LPO, prevented LF accumulation *in vitro* [18] and *in vivo* [19]. Malondialdehyde, a major LPO product, can react with one or two amino groups of macromolecules with the formation of Schiff bases, which undergo Maillard-type intramolecular rearrangements and account for LF fluorescence at 450-470 nm (with the excitation maximum at 360-390 nm) [20]. The formation of aldehyde bridges is a critical mechanism of protein–protein and protein–lipid cross-linking during the generation and progressive "growth" of LF aggregates.

Over the past decade, the studies of LPO have been greatly stimulated by the discovery of ferroptosis, a form of regulated cell death that depends on the iron-catalyzed LPO in cellular membranes [21]. It has been found that ferroptosis contributes to numerous pathologies associated with oxidative stress, including ischemic injury of the heart, brain, and kidneys, as well as neurodegenerative disorders [22]. The interest in ferroptosis has been further fueled by the ability of its inducers to act as anticancer agents capable of overcoming tumor resistance linked to the suppression of apoptosis [23]. The first identified specific inducer of ferroptosis was erastin, an inhibitor of the cystine transporter SLC7A11 required for glutathione biosynthesis [21]. A more selective and potent inducer is the glutathione peroxidase 4 (GPX4) inhibitor RSL3 [24], whose action does not depend on glutathione levels and, therefore, is less constrained by the cellular metabolic context compared to erastin or inhibitors of glutathione biosynthesis.

Our recent work has shown that LPO in the inner mitochondrial membrane (mitoLPO) is essential for ferroptosis [25-28]. We found that erastin triggers mitoLPO, which precedes ferroptotic cell death. The mitochondria-targeted antioxidant SkQ1 [10-(6′-plastoquinonyl)decyltriphenylphosphonium bromide] prevented both mitoLPO and erastin-induced cell death. A similar effect was observed for methylene blue (MB), a well-known redox mediator that allows to bypass the electron transfer through the mitochondrial respiratory complex I, thereby suppressing formation of reactive oxygen species (ROS) [29]. We demonstrated that exogenous iron, supplied as ammonium ferric citrate, induced rapid (within 24 h) LF accumulation in rat H9c2 cardiomyoblasts, preceding ferroptosis [27]. In this model, both LF accumulation and mitochondrial LPO were blocked by SkQ1 and MB, highlighting the importance of mitoLPO in the LF formation.

Here, we investigated LF accumulation in H9c2 cells and human fibroblasts treated with erastin and RSL3. Our findings confirm that mitoLPO can drive rapid LF accumulation in cells.

MATERIALS AND METHODS

Cell cultures. Rat H9c2 cardiomyoblasts (ECACC; cat. no. 88092904) and primary human subcutaneous fibroblasts (Biobank Shared Research Facility, Research Centre for Medical Genetics, Moscow, Russia) were cultured in Dulbecco's Modified Eagle's Medium (DMEM) (Gibco, USA) supplemented with 2 mM L-glutamine, 10% fetal bovine serum (FBS) (HyClone, USA), 100 U/mL penicillin, and 100 U/mL streptomycin (Gibco). Cell viability was assessed using the CellTiterBlue® assay (Promega, USA) according to the manufacturer's protocol. Optical density at 590 nm was measured with a Fluoroskan Ascent FL microplate reader (Thermo Labsystems, USA).

MitoLPO assay. MitoLPO was assessed using the ratiometric fluorescent probe MitoCLox derived from the well-established indicator C11-BODIPY581/591, which specifically reacts with lipid peroxyl radicals, resulting in the shift in its fluorescence spectrum [29]. The cells were incubated with 5 μM erastin or 100 nM RSL3 for 18 h in the presence of 200 nM MitoCLox.

After incubation, the cells were detached using trypsin/EDTA, centrifuged (900*g*, 5 min, 4°C), resuspended in 50 µL PBS, and analyzed by imaging flow cytometry using an Amnis FlowSight cytometer (Luminex Corporation, USA) with excitation at 488 nm and emission at 505-560 nm (Channel 2, Ch2) and 595-642 nm (Channel 4, Ch4). Oxidation of MitoCLox was quantified as the Ch2/Ch4 fluorescence intensity ratio. The data were processed using the Amnis IDEAS® software version 6.2 (Luminex). At least 4000 events were recorded per sample. In cases where signal distribution deviated significantly from Gaussian, gating procedures were applied for accurate data evaluation.

Measurement of cellular LF content. The cells were seeded in 12-well plates. After incubation for 24 h, 5 µM erastin or 100 nM RSL3 were added, either alone or in combination with 100 nM SkQ1, 250 nM MB, 100 µM deferoxamine (DFO), or 200 µM Trolox. LF autofluorescence was detected by flow cytometry (excitation at 488 nm, emission at 505-560 nm, Ch2) [30]. The data were analyzed with the Amnis IDEAS® 6.2 software.

The LF content in H9c2 cells was additionally assessed after seeding the cells in 6-well plates for 18 h, followed by treatment with 100 nM RSL3, with or without 100 nM SkQ1, 250 nM MB, 100 µM DFO, or 200 µM Trolox. After 18-h incubation, the cells were lysed in 1% SDS, and fluorescence spectra were recorded at 500-650 nm (excitation at 405 nm) in a FluoroMax-3 spectrofluorometer (Horiba Scientific, Japan); fluorescence spectra of 1% SDS solution were subtracted from the recorded spectra.

Measurement of cytosolic and mitochondrial ROS. Cytosolic ROS levels were determined using dichlorodihydrofluorescein diacetate (H_2DCFDA) (Invitrogen Life Technologies, USA), while mitochondrial ROS were measured with MitoSOX (Invitrogen Life Technologies). The cells were treated with 5 µM erastin or 100 nM RSL3 for 18 h, followed by incubation in fresh medium containing 1.8 µM H_2DCF-DA or 1 µM MitoSOX for 30 min. Fluorescence was measured using an Amnis FlowSight cytometer with excitation at 488 nm and emission collected in Ch2.

LF content in isolated mitochondria. Mitochondria were isolated from rat hearts in a buffer containing 5 mM MOPS-KOH (pH 7.4), 250 mM sucrose, 1 mM EGTA, and 0.5 mg/mL bovine serum albumin. Cardiac tissue was minced in ice-cold isolation buffer (10 mL/g tissue) and homogenized in a Potter glass homogenizer for 1-2 min. The homogenates were diluted to 20 mL/g tissue and centrifuged at 600*g* for 10 min. The supernatants were collected and centrifuged at 12,000*g* for 10 min. The pellets were resuspended in a minimal volume of the buffer, re-homogenized, diluted with 20 mL of the isolation buffer, and centrifuged again (10 min, 12,000*g*). The final pellets were resuspended and stored on ice.

Mitochondria were incubated in a medium containing 50 µM $FeSO_4$, 5 mM glutamate, 5 mM malate, and 10 µM rotenone at 37°C with constant stirring [1]. Protein concentration was adjusted to 0.4 mg/mL (according to Bradford assay). LF fluorescence was measured after the mitochondria were lysed in 1% SDS at 365-600 nm (excitation at 360 nm) with a FluoroMax-3 spectrofluorometer. MitoCLox oxidation was assessed as described previously [30].

Statistical data processing. The data are presented as mean ± standard deviation (SD) from at least three independent experiments and compared using one-way ANOVA. Statistical significance was evaluated with the Prism 10.0 software (GraphPad Software, USA). The differences were considered significant at **** $p \le 0.0001$, *** $p \le 0.001$, ** $0.001 < p \le 0.05$, and * $p < 0.05$.

RESULTS

Previously, we demonstrated that erastin induced mitoLPO in SV40-transformed MRC5 human lung fibroblasts [25]. The data presented in Fig. 1 show that mitoLPO (measured using MitoCLox) also occurred in rat H9c2 cardiomyoblasts and non-transformed primary human dermal fibroblasts treated with either erastin or RSL3. In all models employed, mitoLPO preceded necrotic cell death. The mitochondria-targeted antioxidant SkQ1 and the redox mediator MB efficiently prevented both mitoLPO and cell death (Fig. 1). Similarly, the cell-permeable iron chelator DFO and the lipophilic antioxidant Trolox exerted protective effects.

Measuring the levels of mitochondrial ROS with the MitoSOX probe revealed that ROS accumulation in our cellular models occurred concomitantly with mitoLPO following the treatment with either erastin or RSL3 (Fig. 2a). We also observed ROS accumulation in the cytoplasm, as assessed with H_2DCFDA (Fig. 2b). In both compartments, ROS accumulation was prevented by the same agents that inhibited mitoLPO.

LF accumulation assessed by flow cytometry based on its broad autofluorescence spectrum (505-560 nm), was observed within the same 18-h timeframe as mitoLPO and preceded cell death (Fig. 3). SkQ1 and MB, as well as DFO and Trolox, completely blocked LF accumulation. The measurements of fluorescence spectra in cell lysates following cell disruption with a detergent confirmed LF accumulation (Fig. 3, d and e). Fluorescence microscopy revealed no formation of LF granules or preferential LF accumulation in the mitochondria.

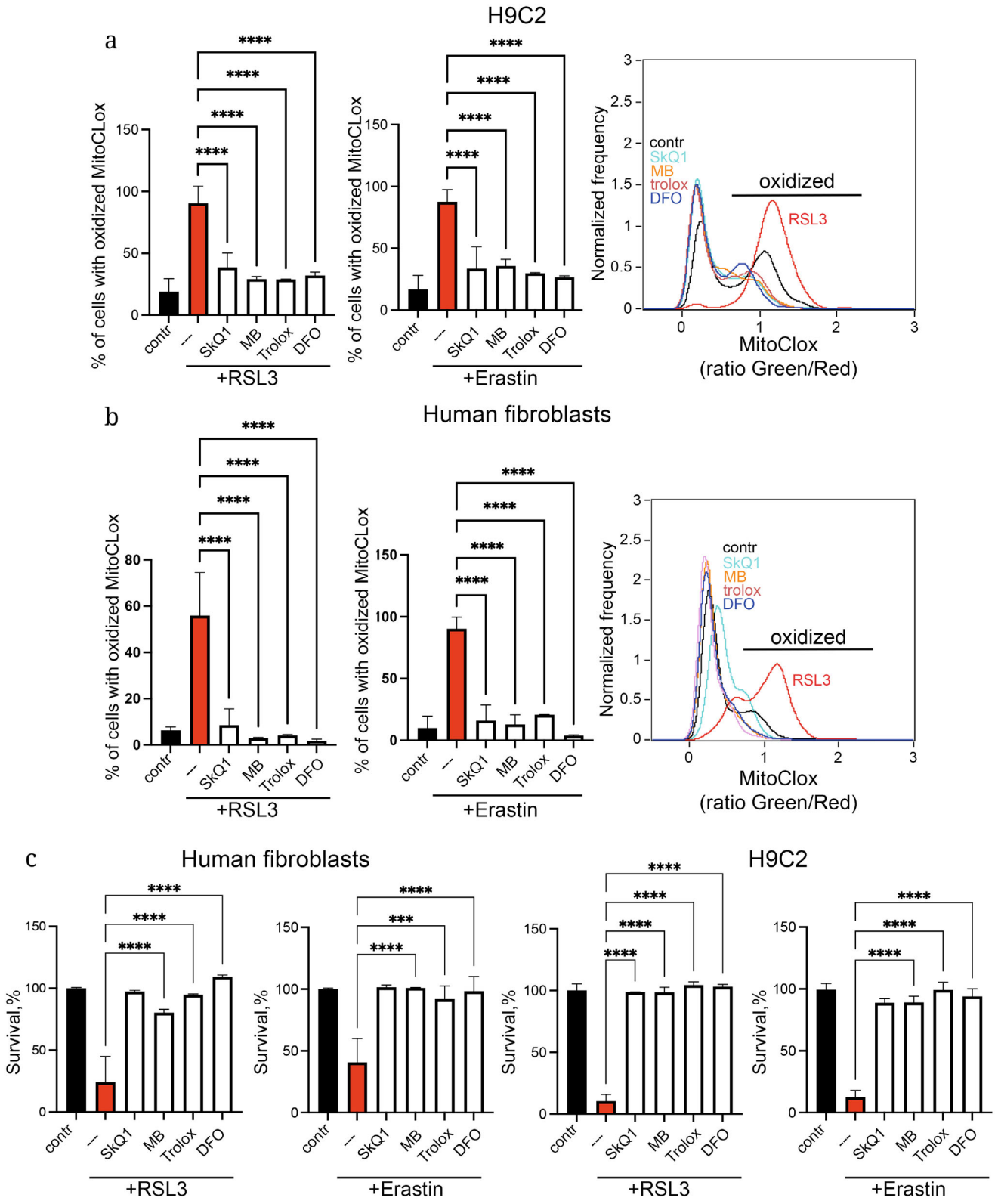

Fig. 1. Erastin and RSL3 induced mitoLPO in rat H9c2 cardiomyoblasts (a) and primary human fibroblasts (b), as well as cell death (c). Cells were incubated with 5 μM erastin or 100 nM RSL3, alone or in combination with 100 nM SkQ1, 250 nM MB, 100 μM DFO, or 200 μM Trolox for 18 h. MitoLPO was assessed by adding ratiometric fluorescent probe MitoCLox to the medium. The ratio of green (Ch2) to red (Ch4) fluorescence was calculated using Amnis IDEAS® 6.2 software. Statistical significance: **** $p < 0.0001$ and *** $p \leq 0.001$, differences between cells treated with erastin or RSL3 and all other treatment conditions (n = 4-6).

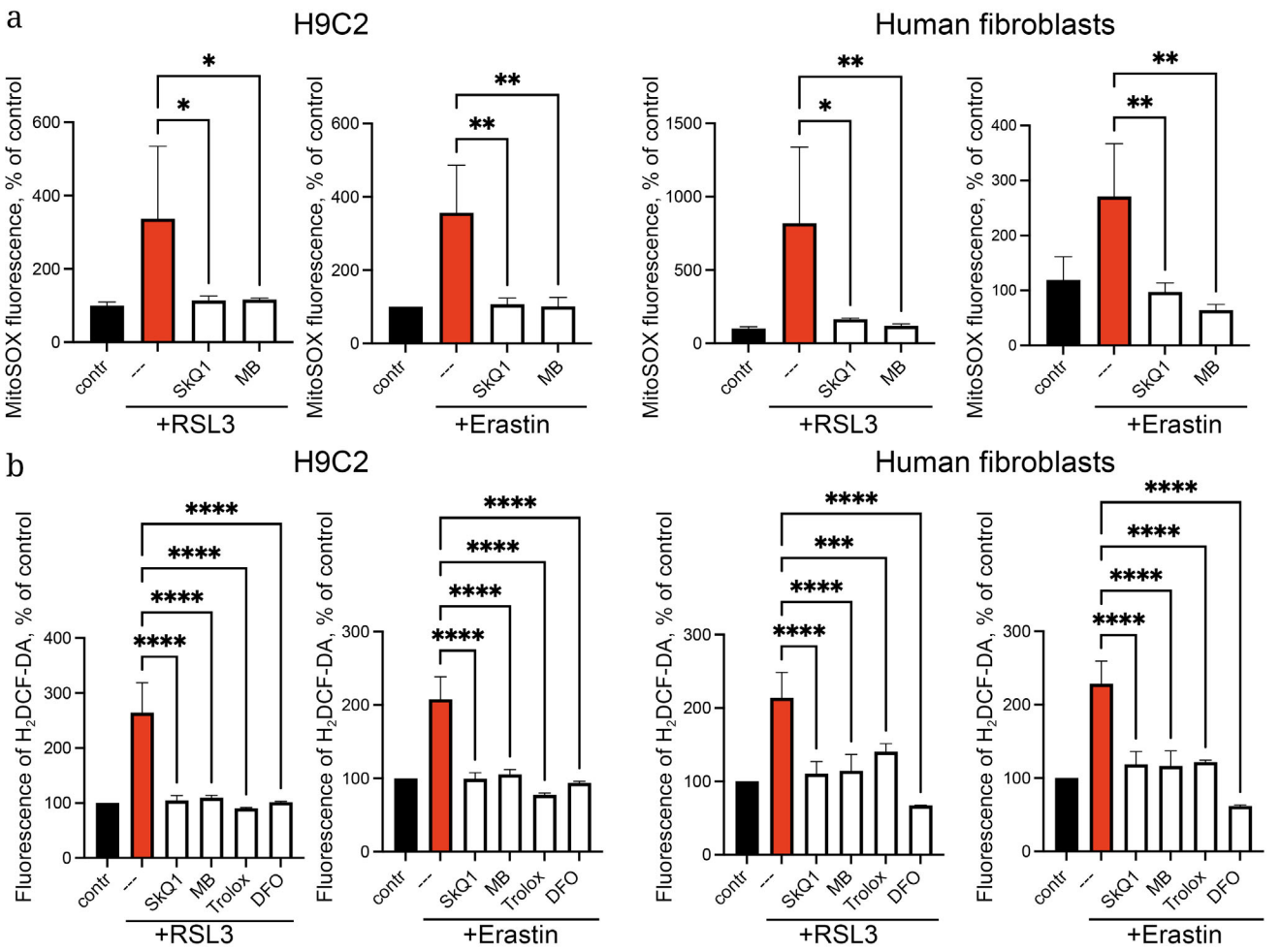

Fig. 2. Erastin and RSL3 induced the formation of (a) mitochondrial superoxide anion (cell staining with 1 μM MitoSOX for 30 min) and (b) cytosolic ROS (cells staining with 1.8 μM H_2DCFDA for 30 min) in H9c2 cardiomyoblasts and primary human fibroblasts. In both cases, the cells were preincubated for 18 h with 5 μM erastin or 100 nM RSL3, alone or in combination with 100 nM SkQ1, 250 nM MB, 100 μM DFO, or 200 μM Trolox. The data are shown as mean fluorescence intensity (% of control). Statistical significance: **** $p < 0.0001$; *** $p \le 0.001$; ** $0.001 < p \le 0.05$; * $p < 0.05$ vs. cells treated with erastin or RSL3.

Interestingly, two distinct subpopulations differing markedly in the level of mitoLPO were observed in the RSL3-treated fibroblasts (Fig. 1). A similar heterogeneity in mitoLPO had previously been detected in SV40-transformed MRC5 fibroblasts exposed to erastin [25]. In H9c2 cells, the heterogeneity was considerably less pronounced (Fig. 1), and the LF accumulation assay revealed population heterogeneity only in fibroblasts (Fig. 3c). The nature of this heterogeneity remains unclear.

In our previous studies [25, 27, 28], we investigated LPO in isolated rat heart mitochondria using MitoCLox. It was found that LPO occurred only in the presence of ferrous ions (Fe^{2+}), while addition of the complex I inhibitor rotenone in the presence of NAD-linked substrates (glutamate and malate) markedly stimulated oxidation, consistent with the LPO induction by ROS generated in complex I. Fluorescence measurements after disruption of the mitochondria with a detergent demonstrated detectable LF accumulation within 24 h at 37°C, which further increased after incubation for additional 24 h (Fig. 4a). Notably, under these conditions, LPO developed within 1-2 h (Fig. 4b), substantially preceding LF accumulation. No LF accumulation was observed in the absence of Fe^{2+} ions. Rotenone promoted LF formation, whereas SkQ1 blocked it, thus highlighting the role of complex I-derived ROS (Fig. 4a).

Earlier studies [31] reported that the LF formation in the mitochondria isolated from rat liver occurred much faster than in the lysosomes or microsomes (membrane vesicles derived from disrupted endoplasmic reticulum). However, preparations of liver mitochondria obtained by differential centrifugation (as in [31]) are unavoidably contaminated with peroxisomes, which contain lipolytic enzymes.

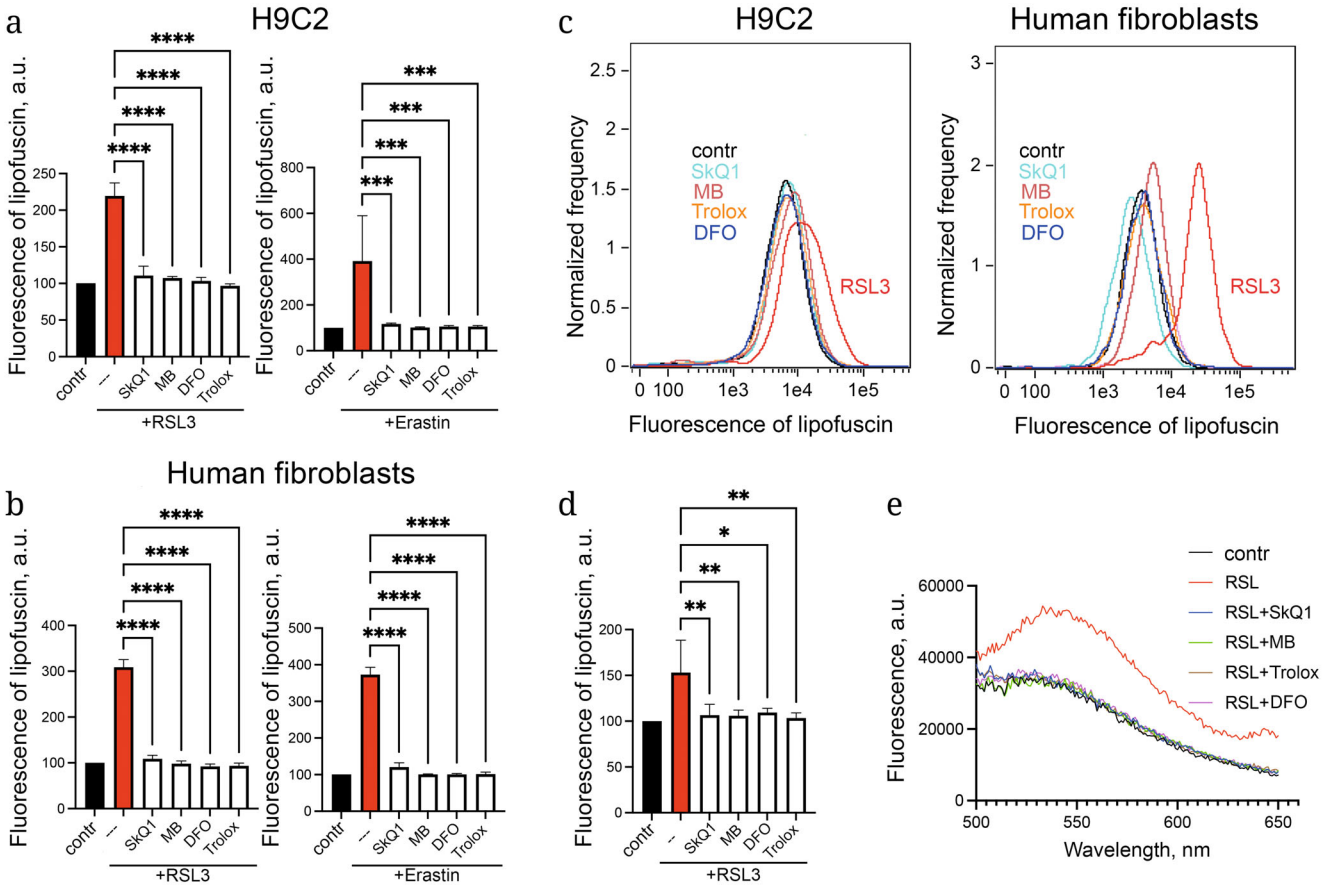

Fig. 3. Effects of erastin and RSL3 on the LF content in H9c2 cells (a) and primary human fibroblasts (b). Cells were incubated for 18 h with 5 μM erastin or 100 nM RSL3, alone or in combination with 100 nM SkQ1, 250 nM MB, 100 μM DFO, or 200 μM Trolox. LF fluorescence was recorded by flow cytometry at 505-560 nm (Ch2) (a, b, and c). LF accumulation was further confirmed after cell lysis with 1% SDS, followed by spectrofluorimetry (d and e). Statistical significance: **** $p < 0.0001$; *** $p \le 0.001$; ** $0.001 < p \le 0.05$; * $p < 0.05$ vs. cells treated with erastin or RSL3.

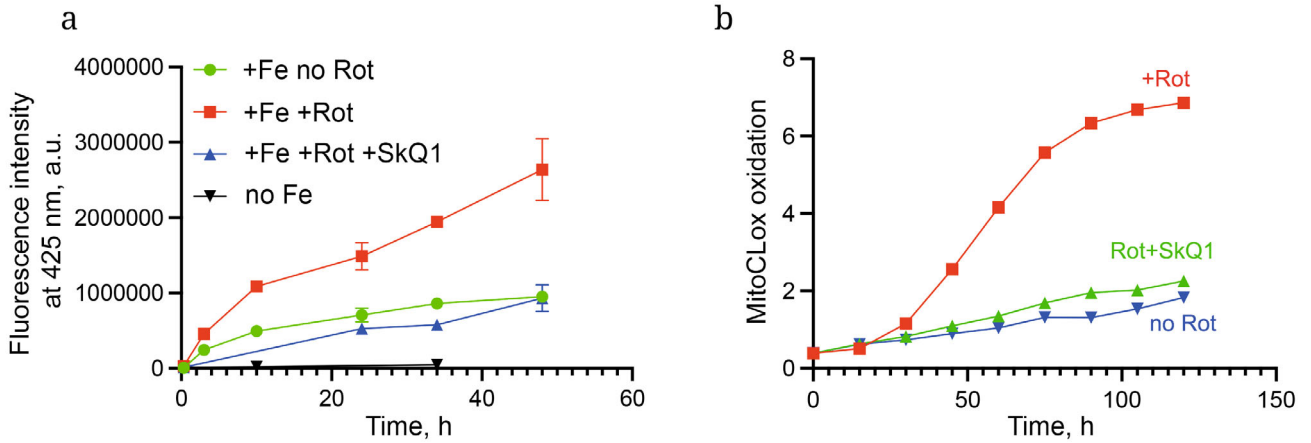

Fig. 4. LF accumulation (a) and LPO rate (b) in isolated rat heart mitochondria. The incubation medium contained $FeSO_4$ (50 μM), glutamate (5 mM), malate (5 mM), rotenone (Rot, 10 μM), and SkQ1 (100 nM).

This contamination may explain the detection of LF in the supernatant following mitochondrial sedimentation at 12,000*g* [31]. The concerns about peroxisomal contamination also extend to a later study [32], which reported accelerated LF formation in liver mitochondria upon heating or UV irradiation. In our experiments on heart mitochondria, the risk of peroxisomal contamination was minimal. The use of detergent disruption in these experiments allowed LF quantification independently of its membrane association.

DISCUSSION

The data presented in Figs. 1 and 3 demonstrate that the activation of mitoLPO by the cystine transport inhibitor erastin or the GPX4 inhibitor RSL3 was accompanied by LF accumulation. The mitochondria-targeted antioxidant SkQ1 and the redox mediator MB, which prevents ROS formation in complex I of the mitochondrial respiratory chain, blocked both mitoLPO and LF accumulation. Previously, we showed [27] that the exogenous iron-induced LF accumulation in H9c2 cells was also inhibited by SkQ1 and MB. These findings indicate that mitoLPO acts as a driving force of accelerated LF formation. Consistent with this conclusion, another mitochondria-targeted antioxidant, MitoTEMPO, was reported to suppress LF accumulation in fibroblasts chronically (for 10 days) treated with the prooxidant paraquat [33]. In the same model, the inhibitor of mitochondrial fragmentation and mitophagy Mdivi-1 promoted LF accumulation, further indicating the critical role of mitochondria in LF biogenesis.

It should be noted that in our experiments, SkQ1 and MB suppressed ROS accumulation in both mitochondria and the cytoplasm (Fig. 2). Hence, we cannot exclude the possibility that ROS generated in the mitochondria contribute to the LF formation alongside LPO products. At the same time, one of the LF inducers used in our study was RSL3, which specifically blocks a defense mechanism against LPO. While erastin can disrupt multiple antioxidant systems through glutathione depletion, GPX4 inhibition selectively promotes LPO without impairing other cellular defenses. Further supporting the view that cellular ROS accumulation results from LPO, DFO (an iron chelator that selectively blocks LPO) prevented ROS accumulation (Fig. 2).

Our data show an important role of mitochondria in the LF formation but do not prove that mitochondria themselves constitute the primary substrate for LF, as fluorescence microscopy revealed no detectable LF accumulation in the mitochondria in our models. However, it is well established that oxidized mitochondria are targeted for mitophagy [34], so LF accumulation in the mitochondria may be transient. Experiments with isolated rat heart mitochondria (Fig. 4) demonstrated rapid LF formation that was markedly accelerated by ROS generated in complex I of the respiratory chain. Additional evidence for the mitochondrial involvement in LF biogenesis comes from the experiments where selective inhibition of the mitochondrial protease Lon in HeLa cells promoted LF accumulation under chronic paraquat treatment [33]. Nevertheless, it remains possible that LPO and protein oxidation in mitochondria trigger LF formation from other cellular components.

LF accumulation occurs not only during physiological aging but also in various diseases, such as age-related macular degeneration (AMD) [35], Stargardt disease (the most common form of inherited juvenile macular degeneration) [36], Alzheimer's disease [37], Parkinson's disease [38], and other neurodegenerative disorders [39]. The pathogenic role of LF has been best established in AMD [5] and Stargardt disease [40], in which LF-containing retinaldehyde dimers (A2E) contribute to the RPE damage via photodynamic effects. Mitochondrial dysfunction has been implicated in AMD pathogenesis [41], and SkQ1 demonstrated therapeutic efficacy in this context [42, 43]. Remofuscin (soraprazan), the first and so far, only pharmacological inhibitor of LF accumulation, has been proposed for the treatment of Stargardt disease [40]. Although the precise mechanism of its action remains unclear, the studies in *Caenorhabditis elegans* showed that remofuscin reduced age-dependent LF accumulation and increased nematode lifespan by 20% [44]. LF-loaded neurons appear to be more susceptible to pathological changes in the Alzheimer's [39] and Parkinson's [45] diseases. The role of mitochondrial dysfunction in neurodegeneration is widely discussed [46]. SkQ1 significantly attenuated progression of the Alzheimer's [47] and Parkinson's [32] disease symptoms in various animal models.

Taken together, our results suggest that mitochondria-targeted compounds can reduce LF accumulation in cells, providing a rationale for their potential therapeutic application in a broad spectrum of conditions associated with excessive LF deposition.

Abbreviations

DFO	deferoxamine
LF	lipofuscin
MB	methylene blue
mitoLPO	mitochondrial lipid peroxidation
LPO	lipid peroxidation
ROS	reactive oxygen species
RPE	retinal pigment epithelium
SkQ1	10-(6′-plastoquinonyl)decyltriphenylphosphonium bromide

Acknowledgments

We thank the Moscow State University Development Program PNR5 for access to the Amnis FlowSight cytometer and Olympus IX83 microscope.

Contributions

B.V.Ch. and K.G.L. developed the concept and supervised the study; H.H., A.A.P., R.A.S., A.V.A., and K.G.L. conducted the experiments; B.V.Ch. and K.G.L. analyzed the data; B.V.Ch. and K.G.L. wrote the draft; H.H. and K.G.L. edited the manuscript.

Funding
This work was supported by the Russian Science Foundation (grant № 23-14-00061). The experimental part of the work was supported by the Russian Science Foundation (grant № 23-14-00061). Data analysis, processing of results, and preparation of the article text were carried out as part of a state assignment from Lomonosov Moscow State University (topic No. AAAA-A19-119031390114-5).

Ethics approval and consent to participate
All animal procedures and experiments were conducted in accordance with international guidelines for the care and use of laboratory animals and were approved by the Institutional Ethics Committee of the Belozersky Institute of Physico-Chemical Biology, Moscow State University (protocol no. 012-5/05/2024, March 24, 2024).

Conflict of interest
The authors of this work declare that they have no conflicts of interest.

REFERENCES

1. Hannover, A. (1842) Mikroskopiske undersögelser af nervesystemet, *Kabernes Selkobs Naturv. Math. Afh. Copenhagen*, **10**, 1-112.
2. Hohn, A., Jung, T., Grimm, S., and Grune, T. (2010) Lipofuscin-bound iron is a major intracellular source of oxidants: role in senescent cells, *Free Radic. Biol. Med.*, **48**, 1100-1108, https://doi.org/10.1016/j.freeradbiomed.2010.01.030.
3. Lee, F. Y., Lee, T. S., Pan, C. C., Huang, A. L., and Chau, L. Y. (1998) Colocalization of iron and ceroid in human atherosclerotic lesions, *Atherosclerosis*, **138**, 281-288, https://doi.org/10.1016/S0021-9150(98)00033-1.
4. Ablonczy, Z., Smith, N., Anderson, D. M., Grey, A. C., Spraggins, J., Koutalos, Y., Schey, K. L., and Crouch, R. K. (2014) The utilization of fluorescence to identify the components of lipofuscin by imaging mass spectrometry, *Proteomics*, **14**, 936-944, https://doi.org/10.1002/pmic.201300406.
5. Feldman, T. B., Dontsov, A. E., Yakovleva, M. A., and Ostrovsky, M. A. (2022) Photobiology of lipofuscin granules in the retinal pigment epithelium cells of the eye: norm, pathology, age, *Biophys. Rev.*, **14**, 1051-1065, https://doi.org/10.1007/s12551-022-00989-9.
6. Hohn, A., Sittig, A., Jung, T., Grimm, S., and Grune, T. (2012) Lipofuscin is formed independently of macroautophagy and lysosomal activity in stress-induced prematurely senescent human fibroblasts, *Free Radic. Biol. Med.*, **53**, 1760-1769, https://doi.org/10.1016/j.freeradbiomed.2012.08.591.
7. Ivy, G. O., Kanai, S., Ohta, M., Smith, G., Sato, Y., Kobayashi, M., and Kitani, K. (1989) Lipofuscin-like substances accumulate rapidly in brain, retina and internal organs with cysteine protease inhibition, *Adv. Exp. Med. Biol.*, **266**, 31-45, https://doi.org/10.1007/978-1-4899-5339-1_3.
8. Terman, A., Kurz, T., Navratil, M., Arriaga, E. A., and Brunk, U. T. (2010) Mitochondrial turnover and aging of long-lived postmitotic cells: the mitochondrial-lysosomal axis theory of aging, *Antioxid. Redox Signal.*, **12**, 503-535, https://doi.org/10.1089/ars.2009.2598.
9. Ottis, P., Koppe, K., Onisko, B., Dynin, I., Arzberger, T., Kretzschmar, H., Requena, J. R., Silva, C. J., Huston, J. P., and Korth, C. (2012) Human and rat brain lipofuscin proteome, *Proteomics*, **12**, 2445-2454, https://doi.org/10.1002/pmic.201100668.
10. Li, W. W., Wang, H. J., Tan, Y. Z., Wang, Y. L., Yu, S. N., and Li, Z. H. (2021) Reducing lipofuscin accumulation and cardiomyocytic senescence of aging heart by enhancing autophagy, *Exp. Cell Res.*, **403**, 112585, https://doi.org/10.1016/j.yexcr.2021.112585.
11. Walter, S., Haseli, S. P., Baumgarten, P., Deubel, S., Jung, T., Hohn, A., Ott, C., and Grune, T. (2025) Oxidized protein aggregate lipofuscin impairs cardiomyocyte contractility via late-stage autophagy inhibition, *Redox Biol.*, **81**, 103559, https://doi.org/10.1016/j.redox.2025.103559.
12. Davies, S., Elliott, M. H., Floor, E., Truscott, T. G., Zareba, M., Sarna, T., Shamsi, F. A., and Boulton, M. E. (2001) Photocytotoxicity of lipofuscin in human retinal pigment epithelial cells, *Free Radic. Biol. Med.*, **31**, 256-265, https://doi.org/10.1016/S0891-5849(01)00582-2.
13. Baldensperger, T., Jung, T., Heinze, T., Schwerdtle, T., Hohn, A., and Grune, T. (2024) The age pigment lipofuscin causes oxidative stress, lysosomal dysfunction, and pyroptotic cell death, *Free Radic. Biol. Med.*, **225**, 871-880, https://doi.org/10.1016/j.freeradbiomed.2024.10.311.

14. Porta, E., Llesuy, S., Monserrat, A. J., Benavides, S., and Travacio, M. (1995) Changes in cathepsin B and lipofuscin during development and aging in rat brain and heart, *Gerontology*, **41**, 81-93, https://doi.org/10.1159/000213727.
15. Nakano, M., Oenzil, F., Mizuno, T., and Gotoh, S. (1995) Age-related changes in the lipofuscin accumulation of brain and heart, *Gerontology*, **41**, 69-79, https://doi.org/10.1159/000213726.
16. Kakimoto, Y., Okada, C., Kawabe, N., Sasaki, A., Tsukamoto, H., Nagao, R., and Osawa, M. (2019) Myocardial lipofuscin accumulation in ageing and sudden cardiac death, *Sci. Rep.*, **9**, 3304, https://doi.org/10.1038/s41598-019-40250-0.
17. Faragher, R. G. A. (2021) Simple detection methods for senescent cells: opportunities and challenges, *Front. Aging*, **2**, 686382, https://doi.org/10.3389/fragi.2021.686382.
18. Barbouti, A., Lagopati, N., Veroutis, D., Goulas, V., Evangelou, K., Kanavaros, P., Gorgoulis, V. G., and Galaris, D. (2021) Implication of dietary iron-chelating bioactive compounds in molecular mechanisms of oxidative stress-induced cell ageing, *Antioxidants (Basel)*, **10**, 491, https://doi.org/10.3390/antiox10030491.
19. Naseri, N. N., Ergel, B., Kharel, P., Na, Y., Huang, Q., Huang, R., Dolzhanskaya, N., Burre, J., Velinov, M. T., and Sharma, M. (2020) Aggregation of mutant cysteine string protein-alpha via Fe-S cluster binding is mitigated by iron chelators, *Nat. Struct. Mol. Biol.*, **27**, 192-201, https://doi.org/10.1038/s41594-020-0375-y.
20. Yin, D. (1996) Biochemical basis of lipofuscin, ceroid, and age pigment-like fluorophores, *Free Radic. Biol. Med.*, **21**, 871-888, https://doi.org/10.1016/0891-5849(96)00175-X.
21. Dixon, S. J., Lemberg, K. M., Lamprecht, M. R., Skouta, R., Zaitsev, E. M., Gleason, C. E., Patel, D. N., Bauer, A. J., Cantley, A. M., Yang, W. S., Morrison, B., 3rd, and Stockwell, B. R. (2012) Ferroptosis: an iron-dependent form of nonapoptotic cell death, *Cell*, **149**, 1060-1072, https://doi.org/10.1016/j.cell.2012.03.042.
22. Berndt, C., Alborzinia, H., Amen, V. S., Ayton, S., Barayeu, U., Bartelt, A., Bayir, H., Bebber, C. M., Birsoy, K., Bottcher, J. P., Brabletz, S., Brabletz, T., Brown, A. R., Brune, B., Bulli, G., Bruneau, A., Chen, Q., DeNicola, G. M., Dick, T. P., Distefano, A., Dixon, S. J., Engler, J. B., Esser-von Bieren, J., Fedorova, M., Friedmann Angeli, J. P., Friese, M. A., Fuhrmann, D. C., Garcia-Saez, A. J., Garbowicz, K., Gotz, M., Gu, W., Hammerich, L., Hassannia, B., Jiang, X., Jeridi, A., Kang, Y. P., Kagan, V. E., Konrad, D. B., Kotschi, S., Lei, P., Le Tertre, M., Lev, S., Liang, D., Linkermann, A., Lohr, C., Lorenz, S., Luedde, T., Methner, A., Michalke, B., Milton, A. V., Min, J., Mishima, E., Muller, S., Motohashi, H., Muckenthaler, M. U., Murakami, S., Olzmann, J. A., Pagnussat, G., Pan, Z., Papagiannakopoulos, T., Pedrera Puentes, L., Pratt, D. A., Proneth, B., Ramsauer, L., Rodriguez, R., Saito, Y., Schmidt, F., Schmitt, C., Schulze, A., Schwab, A., Schwantes, A., Soula, M., Spitzlberger, B., Stockwell, B. R., Thewes, L., Thorn-Seshold, O., Toyokuni, S., Tonnus, W., Trumpp, A., Vandenabeele, P., Vanden Berghe, T., Venkataramani, V., Vogel, F. C. E., von Karstedt, S., Wang, F., Westermann, F., Wientjens, C., Wilhelm, C., Wolk, M., Wu, K., Yang, X., Yu, F., Zou, Y., and Conrad, M. (2024) Ferroptosis in health and disease, *Redox Biol.*, **75**, 103211, https://doi.org/10.1016/j.redox.2024.103211.
23. Stockwell, B. R. (2022) Ferroptosis turns 10: emerging mechanisms, physiological functions, and therapeutic applications, *Cell*, **185**, 2401-2421, https://doi.org/10.1016/j.cell.2022.06.003.
24. Yang, W. S., SriRamaratnam, R., Welsch, M. E., Shimada, K., Skouta, R., Viswanathan, V. S., Cheah, J. H., Clemons, P. A., Shamji, A. F., Clish, C. B., Brown, L. M., Girotti, A. W., Cornish, V. W., Schreiber, S. L., and Stockwell, B. R. (2014) Regulation of ferroptotic cancer cell death by GPX4, *Cell*, **156**, 317-331, https://doi.org/10.1016/j.cell.2013.12.010.
25. Lyamzaev, K. G., Panteleeva, A. A., Simonyan, R. A., Avetisyan, A. V., and Chernyak, B. V. (2023) Mitochondrial lipid peroxidation is responsible for ferroptosis, *Cells*, **12**, 611, https://doi.org/10.3390/cells12040611.
26. Huan, H., Lyamzaev, K. G., Panteleeva, A. A., and Chernyak, B. V. (2024) Mitochondrial lipid peroxidation is necessary but not sufficient for induction of ferroptosis, *Front. Cell Dev. Biol.*, **12**, 1452824, https://doi.org/10.3389/fcell.2024.1452824.
27. Lyamzaev, K. G., Huan, H., Panteleeva, A. A., Simonyan, R. A., Avetisyan, A. V., and Chernyak, B. V. (2024) Exogenous iron induces mitochondrial lipid peroxidation, lipofuscin accumulation, and ferroptosis in H9c2 cardiomyocytes, *Biomolecules*, **14**, 730, https://doi.org/10.3390/biom14060730.
28. Lyamzaev, K. G., Panteleeva, A. A., Simonyan, R. A., Avetisyan, A. V., and Chernyak, B. V. (2023) The critical role of mitochondrial lipid peroxidation in ferroptosis: insights from recent studies, *Biophys. Rev.*, **15**, 875-885, https://doi.org/10.1007/s12551-023-01126-w.
29. Pap, E. H., Drummen, G. P., Winter, V. J., Kooij, T. W., Rijken, P., Wirtz, K. W., Op den Kamp, J. A., Hage, W. J., and Post, J. A. (1999) Ratio-fluorescence microscopy of lipid oxidation in living cells using C11-BODIPY(581/591), *FEBS Lett.*, **453**, 278-282, https://doi.org/10.1016/S0014-5793(99)00696-1.
30. Malavolta, M., Giacconi, R., Piacenza, F., Strizzi, S., Cardelli, M., Bigossi, G., Marcozzi, S., Tiano, L., Marcheggiani, F., Matacchione, G., Giuliani, A., Olivieri, F., Crivellari, I., Beltrami, A. P., Serra, A., Demaria, M., and Provinciali, M. (2022) Simple detection of unstained live senescent cells with imaging flow cytometry, *Cells*, **11**, 2506, https://doi.org/10.3390/cells11162506.

31. Chio, K. S., Reiss, U., Fletcher, B., and Tappel, A. L. (1969) Peroxidation of subcellular organelles: formation of lipofuscinlike fluorescent pigments, *Science*, **166**, 1535-1536, https://doi.org/10.1126/science.166.3912.1535.
32. Pavshintsev, V. V., Podshivalova, L. S., Frolova, O. Y., Belopolskaya, M. V., Averina, O. A., Kushnir, E. A., Marmiy, N. V., and Lovat, M. L. (2017) Effects of mitochondrial antioxidant SkQ1 on biochemical and behavioral parameters in a Parkinsonism model in mice, *Biochemistry (Moscow)*, **82**, 1513-1520, https://doi.org/10.1134/S0006297917120100.
33. Konig, J., Ott, C., Hugo, M., Jung, T., Bulteau, A. L., Grune, T., and Hohn, A. (2017) Mitochondrial contribution to lipofuscin formation, *Redox Biol.*, **11**, 673-681, https://doi.org/10.1016/j.redox.2017.01.017.
34. Picca, A., Faitg, J., Auwerx, J., Ferrucci, L., and D'Amico, D. (2023) Mitophagy in human health, ageing and disease, *Nat. Metab.*, **5**, 2047-2061, https://doi.org/10.1038/s42255-023-00930-8.
35. Pollreisz, A., Messinger, J. D., Sloan, K. R., Mittermueller, T. J., Weinhandl, A. S., Benson, E. K., Kidd, G. J., Schmidt-Erfurth, U., and Curcio, C. A. (2018) Visualizing melanosomes, lipofuscin, and melanolipofuscin in human retinal pigment epithelium using serial block face scanning electron microscopy, *Exp. Eye Res.*, **166**, 131-139, https://doi.org/10.1016/j.exer.2017.10.018.
36. Huang, D., Heath Jeffery, R. C., Aung-Htut, M. T., McLenachan, S., Fletcher, S., Wilton, S. D., and Chen, F. K. (2022) Stargardt disease and progress in therapeutic strategies, *Ophthalmic Genet.*, **43**, 1-26, https://doi.org/10.1080/13816810.2021.1966053.
37. Stojanovic, A., Roher, A. E., and Ball, M. J. (1994) Quantitative analysis of lipofuscin and neurofibrillary tangles in the hippocampal neurons of Alzheimer disease brains, *Dementia*, **5**, 229-233, https://doi.org/10.1159/000106728.
38. Ulfig, N., Braak, E., and Braak, H. (1989) Changes within the basal nucleus in Parkinson's disease, *Prog. Clin. Biol. Res.*, **317**, 493-500.
39. Moreno-Garcia, A., Kun, A., Calero, O., Medina, M., and Calero, M. (2018) An overview of the role of lipofuscin in age-related neurodegeneration, *Front. Neurosci.*, **12**, 464, https://doi.org/10.3389/fnins.2018.00464.
40. Fang, Y., Taubitz, T., Tschulakow, A. V., Heiduschka, P., Szewczyk, G., Burnet, M., Peters, T., Biesemeier, A., Sarna, T., Schraermeyer, U., and Julien-Schraermeyer, S. (2022) Removal of RPE lipofuscin results in rescue from retinal degeneration in a mouse model of advanced Stargardt disease: Role of reactive oxygen species, *Free Radic. Biol. Med.*, **182**, 132-149, https://doi.org/10.1016/j.freeradbiomed.2022.02.025.
41. Kaarniranta, K., Uusitalo, H., Blasiak, J., Felszeghy, S., Kannan, R., Kauppinen, A., Salminen, A., Sinha, D., and Ferrington, D. (2020) Mechanisms of mitochondrial dysfunction and their impact on age-related macular degeneration, *Prog. Retin. Eye Res.*, **79**, 100858, https://doi.org/10.1016/j.preteyeres.2020.100858.
42. Muraleva, N. A., Kozhevnikova, O. S., Zhdankina, A. A., Stefanova, N. A., Karamysheva, T. V., Fursova, A. Z., and Kolosova, N. G. (2014) The mitochondria-targeted antioxidant SkQ1 restores alphaB-crystallin expression and protects against AMD-like retinopathy in OXYS rats, *Cell Cycle*, **13**, 3499-3505, https://doi.org/10.4161/15384101.2014.958393.
43. Novikova, Y. P., Gancharova, O. S., Eichler, O. V., Philippov, P. P., and Grigoryan, E. N. (2014) Preventive and therapeutic effects of SkQ1-containing Visomitin eye drops against light-induced retinal degeneration, *Biochemistry (Moscow)*, **79**, 1101-1110, https://doi.org/10.1134/S0006297914100113.
44. Oh, M., Yeom, J., Schraermeyer, U., Julien-Schraermeyer, S., and Lim, Y. H. (2022) Remofuscin induces xenobiotic detoxification via a lysosome-to-nucleus signaling pathway to extend the *Caenorhabditis elegans* lifespan, *Sci. Rep.*, **12**, 7161, https://doi.org/10.1038/s41598-022-11325-2.
45. Braak, E., Sandmann-Keil, D., Rub, U., Gai, W. P., de Vos, R. A., Steur, E. N., Arai, K., and Braak, H. (2001) alpha-synuclein immunopositive Parkinson's disease-related inclusion bodies in lower brain stem nuclei, *Acta Neuropathol.*, **101**, 195-201, https://doi.org/10.1007/s004010000247.
46. Klemmensen, M. M., Borrowman, S. H., Pearce, C., Pyles, B., and Chandra, B. (2024) Mitochondrial dysfunction in neurodegenerative disorders, *Neurotherapeutics*, **21**, e00292, https://doi.org/10.1016/j.neurot.2023.10.002.
47. Stefanova, N. A., Muraleva, N. A., Skulachev, V. P., and Kolosova, N. G. (2014) Alzheimer's disease-like pathology in senescence-accelerated OXYS rats can be partially retarded with mitochondria-targeted antioxidant SkQ1, *J. Alzheimers Dis.*, **38**, 681-694, https://doi.org/10.3233/JAD-131034.